



HAL
open science

Intraoperative tracking of aortic valve plane

Duc Long Hung Nguyen, Mireille Garreau, Vincent Auffret, Hervé Le Breton,
Jean-Philippe Verhoye, Pascal Haigron

► **To cite this version:**

Duc Long Hung Nguyen, Mireille Garreau, Vincent Auffret, Hervé Le Breton, Jean-Philippe Verhoye, et al.. Intraoperative tracking of aortic valve plane. 35th Annual International Conference of the IEEE Engineering in Medicine and Biology Society (EMBS), Jul 2013, Osaka, Japan. pp.4378-81, 10.1109/EMBC.2013.6610516 . hal-00869219

HAL Id: hal-00869219

<https://univ-rennes.hal.science/hal-00869219>

Submitted on 2 Oct 2013

HAL is a multi-disciplinary open access archive for the deposit and dissemination of scientific research documents, whether they are published or not. The documents may come from teaching and research institutions in France or abroad, or from public or private research centers.

L'archive ouverte pluridisciplinaire **HAL**, est destinée au dépôt et à la diffusion de documents scientifiques de niveau recherche, publiés ou non, émanant des établissements d'enseignement et de recherche français ou étrangers, des laboratoires publics ou privés.

Intraoperative Tracking of Aortic Valve Plane*

DLH Nguyen, M Garreau, V Auffret, H Le Breton, JP Verhoye, P Haigron

Abstract—The main objective of this work is to track the aortic valve plane in intra-operative fluoroscopic images in order to optimize and secure Transcatheter Aortic Valve Implantation (TAVI) procedure. This paper is focused on the issue of aortic valve calcifications tracking in fluoroscopic images. We propose a new method based on the Tracking-Learning-Detection approach, applied to the aortic valve calcifications in order to determine the position of the aortic valve plane in intra-operative TAVI images. This main contribution concerns the improvement of object detection by updating the recursive tracker in which all features are tracked jointly. The approach has been evaluated on four patient databases, providing an absolute mean displacement error less than 10 pixels ($\approx 2\text{mm}$). Its suitability for the TAVI procedure has been analyzed.

I. INTRODUCTION

Aortic stenosis is the most common valvular lesion occurring among elderly patients and has become extremely frequent because of changing demographics in industrialized countries. Surgical risk after the age of 70 has increased. Transcatheter aortic valve implantation (TAVI) has emerged as a promising alternative to conventional aortic valve replacement for elderly patients with severe, symptomatic aortic stenosis who are otherwise left untreated due to the perceived high risk of operative mortality. Compared to the standard aortic valve replacement surgery, the TAVI limits the surgical access to either a small minithoracotomy (transapical TAVI) or femoral approach (transfemoral TAVI) causing minimal tissue trauma. About the transfemoral artery procedure that is the most common used, after catheterization through a femoral access, the overall procedure consists in introducing the transcatheter valve passing through successively the descending aorta, the ascending aorta and the native valve to finally perform the deployment of the aortic valve bioprosthesis. For both access types, the last stages concerning the localization and the deployment of the valve need the development of efficient tools to make more secure and reliable the TAVI procedure.

Determining exactly valve location and minimizing the use of contrast injections are urgently needed during the surgical intervention, because complications can arise from a misplaced valve. These complications have been reported [1] such as high-degree atrioventricular block (10-30%), paravalvular leak (4-35%), coronary ostia occlusion (0.5-1%), aortic dissection (0-4%) and cardiac tamponade (1-9%). The 30-day mortality of the TAVI in Europe is 5-10% [2]. By comparison, Cribier et al. enrolled patients with a mean predicted operative risk of $12 \pm 2\%$ for TAVI and experienced a 30-day mortality of 18% [3]. Also, the contrast of fluoroscopic images is generally limited to minimize the radiation exposure for both the patient and the physician. The amount of contrast agent that is injected to visualize the aortic root, valve annulus, and coronary ostia in few seconds must be minimized to avoid renal insufficiencies in elderly high-risk patients.

In the intra-operative phase, Angiography - Fluoroscopy is the reference dynamic imaging modality for guiding TAVI. Device positioning during TAVI has to be performed with respect to the native valve plane that remains difficult to observe and determine intra-operatively. Moreover, several angiographic injections are often required due to the lack of navigation tools. The objective is thus to develop efficient tools coping with difficulties in obtaining an optimal view of the native valve to define then an optimal target location.

Only few previous studies deal with image-guided planning and intra-operative support for TAVI procedure. About the Aortic Valve Plane (AVP) tracking, Wijesinghe et al. [4] have previously proposed a system for the tracking of the AVP in fluoroscopic image sequences. Esmail Karar et al. [5] have proposed a system that integrates a 3D aortic mesh model and landmarks from intra-operative C-arm CT images with tracking the prosthesis in live fluoroscopic images by using the pigtail catheter.

*This work was partially supported by the ITEA2 MEDIATE project (ITEA 09039).

DLH Nguyen, P Haigron, M Garreau are with INSERM, U1099, Rennes, F-35000, France and Université de Rennes 1, LTSI, Rennes, F-35000, France; There are also members of CAMI LABEX, France.

H Le Breton, JP Verhoye and V Auffret are with INSERM, U1099, Rennes, F-35000, France, with Université de Rennes 1, LTSI, Rennes, F-35000, France and with CCP, University Hospital Pontchaillou, Rennes, F-35000, France.

In this context, we propose a robust method based on the Tracking-Learning-Detection approach, applied to the aortic valve calcifications in order to determine the position of the aortic valve plane in intra-operative TAVI images. This method allows continuous visualization of diseased valve plane without further contrast injections and despite some difficulties in the images (disappearance of objects, contrast variations). This tracking is based on the joint detection and tracking of the aortic valve calcifications that are considered to be connected to the valve plane and to follow its displacements.

The paper is organized as follows. Section 2 describes the method that we propose to track the aortic valve calcifications. The Section 3 presents experimental results on real data and their quantitative evaluation. Section 4 gives a conclusion and final remarks.

II. METHOD

To assist the TAVI, our tracking procedure is connected with the fluoroscopy system as depicted in Fig. 1. 2D fluoroscopic image sequences are acquired by the tracking system. The AVP procedure is composed of three steps: *Initialization* to generate the calcification template (image in the bounding box of the calcification) and to define the distance between the calcification and the AVP in one chosen frame; *Tracking of Calcifications* to determine the position of calcifications in each frame of the sequence; *Updating of the Aortic Valve Plane* to depict the overlaid AVP onto 2D fluoroscopic images without contrast injections.

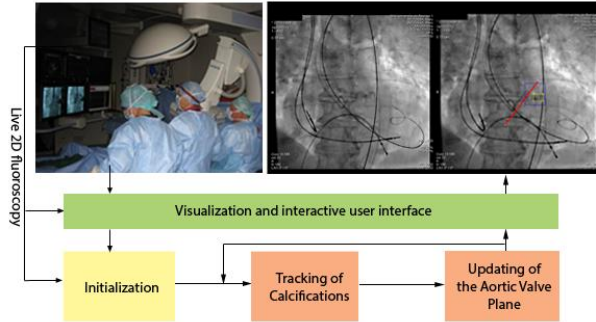


Figure 1. Block diagram of the developed tracking procedure connected with the interventional imaging system for guiding the TAVI.

A. Initialization

In this work, we focus on semi-automated single-target tracking [6]. For the initialization step, a sequence of images $I_0 \dots I_c \dots I_p \dots I_n$ is acquired from the interventional imaging system. In this sequence, I_c and I_p identify frames without and with contrast injections respectively. In order to initialize the tracking process, user input is needed.

Figure 2 presents the key points of initialization steps. The expert who has the best experience and knowledge about the TAVI procedure firstly initializes the calcification in the image I_c (Figure 2a). Then, in the image I_p , the AVP is defined (Figure 2b). The positions of calcification from frame I_c to I_p are automatically determined by the optical flow method (Figure 2c). At the end of the initialization step, the calcification template (image inside the bounding box of the calcification) and the distance from this template and the AVP are used for the two next steps (Figure 2d).

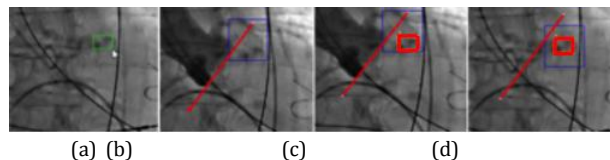


Figure 2. Initialization. (a) The bounding box of calcification is manually initialized; (b) The AVP is defined in the contrast injection image; (c) The rigid link between calcification and AVP is established; (d) The calcification and the AVP are tracked.

In these pictures, the blue box represents the region of interest (ROI) (the research window for the detector and the recursive tracking), the green box shows the initialized bounding box of the

calcification meanwhile the red box denotes the tracked one, the red line is the position of the aortic valve plane.

B. Tracking of Calcifications

After the initialization step, the tracking process is started with training. No further user interaction is required. Figure 3 depicts the workflow of this stage. The detector and the recursive tracker run in parallel and the results from both are fused into a single final result. If this result passes a validation stage, updating of the position of the aortic valve plane is performed. Then, the process repeats from training. Particularly, in the first running of the process, the detector is executed before to initialize the calcification location for the tracker.

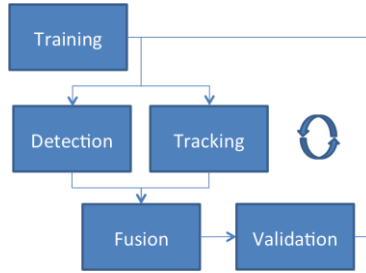


Figure 3. Overall scheme of the tracking process.

In the training step, we used the method proposed by Kalal et al. [7]. We kept separate templates for positive examples of the calcification and for negative examples found in the background. All maintained templates are normalized in brightness and size.

For object detection, these templates form the basis of an object detector that is run independently of the tracker. If the detector finds a location in an image exhibiting a high similarity to the templates, the tracker is re-initialized on this location. Since the comparison of templates is computationally expensive, we employed a cascaded approach to detect the object. Our object detection cascade consists of a variance filter, a random fern classifier based on 2-bit-binary features proposed in [8] and the template matching method.

For the tracking, we applied the approach of Kalal et al. [9]. The input of this tracking concerns the object location in the previous frame given by the detection stage. This approach is based on estimating optical flow using the method of Lucas and Kanade [10]. However, the optical-flow based tracking method is not interior-aware. Each of the bounding box and calcification points are tracked independently, which may result in calcification features leaking out of the bounding box. We used idea from the method of Stanley et al. [11] for the outlier detection and local interpolation to avoid this conflict.

For fusion stage, the results of the confident detections and the recursive tracker are combined into a final result. This final decision is based on the number of detections, on their confidence values and on the confidence of the tracking result. If the detector yields exactly one result with a confidence higher than the result from the recursive tracker, then the response of the detector is assigned to the final result. This corresponds to a re-initialization of the recursive tracker. If the recursive tracker produces a result and is not re-initialized by the detector, the result of the recursive tracker is assigned to the final result. In all other cases the final result remains empty, which suggests that the calcification is not visible in the current frame.

C. Updating of the Aortic Valve Plane

Real-time tracking of the aortic valve plane is performed for each frame of the sequence by calculating the updated displacement of the calcifications between two frames. This displacement is obtained by the difference between the calcification location in one frame and the corresponding calcification position in the other frame. An example of the calcification motion is given in Figure 4: the yellow arrow (with amplitude multiplied by 10 for visibility) is the 2D displacement vector of the calcifications between two frames.

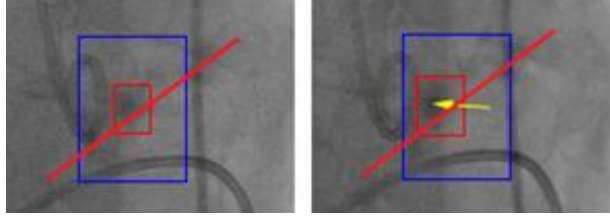


Figure 4. 2D displacement of the calcification. The blue box presents the region of interest (ROI), the red box denotes a bounding box of the calcifications, the red line is the position of the aortic valve plane and the yellow arrow (with amplitude multiplied by 10 for visibility) is the 2D displacement vector of the calcification between two frames.

III. EXPERIMENTAL RESULTS

Our approach has been tested and evaluated on fluoroscopy image sequences that have been previously recorded on real patients during intra-operative TAVI procedures. The acquired fluoroscopic images are of 512x512 pixels (1 pixel \approx 0,2 mm), with a frame rate of 15 images/s and a sequence duration of about 25 s. We employed the recall and precision standard metrics for assessing performance of the tracking process that has been applied on calcifications. For this evaluation, the method has been implemented in C++ and low-level image operations were implemented as function calls to the OpenCV library. All experiments were conducted on an Intel Core 2 Duo CPU T7300 processor running at 2.0 GHz under Ubuntu 11.102. The average execution time is about 65ms for one frame.

A. Evaluation Protocol

1) Recall and Precision metrics

Two performance metrics have been used (“recall” and “precision”) that are based on True Positives (TP), False Positives (FP), True Negatives (TN) and False Negatives (FN) values. These last values are computed from the overlapping of manually defined and detected calcifications templates. After processing each video sequence, all occurrences of TP, FP, TN and FN are counted. Based on these values we calculated the two metrics as:

$$recall = \frac{TP}{TP + FN} \quad (1)$$

Eq. (1) measures the fraction of positive examples that are correctly labeled. Precision is defined as

$$precision = \frac{TP}{TP + FP} \quad (2)$$

Eq. (2) measures the fraction of examples classified as positive that are truly positive.

In our application, both high recall and high precision are required.

2) Displacement Error

In each image of all tested datasets, absolute displacement errors between manually defined and automatically detected positions are computed. These positions correspond to the barycenters of the calcifications bounding boxes. For each image i of the sequence, the automatic localized barycenter (x_i^A, y_i^A) and manual one (x_i^M, y_i^M) were used to compute the Euclidian displacement error d_i . The absolute mean error $d_{mean} \pm$ standard deviation (SD) and maximum error d_{max} were also computed over n images of the sequence.

B. Calcification Tracking Results

Figure 5 represents successive images of one patient sequence (D) with the visualization of the detected calcification template in red color. This figure illustrates that this method is able to track the calcification and detect it again despite the fact that it may disappear in some frames. In the first one (a) and in the second one with the arrival of contrast product (b), the calcification is well localized. In the third one (c), the calcification is lost and in the last one (d), the calcification is detected again.

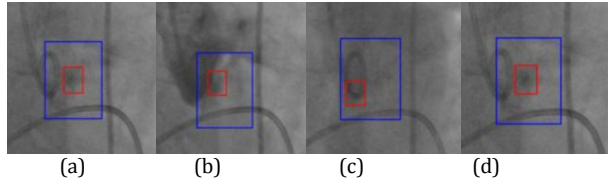


Figure 5. Qualitative results for the sequence D. (a) The calcification is detected, (b) The calcification is well localized with the arrival of contrast inject, (c) The calcification is lost, (d) The calcification is detected again.

The tracked calcification results for the sequence D are presented in Fig. 6 and Fig. 7. The barycenter spatial position is represented on X-axis (Figure 6) and on Y-axis (Figure 7) with a comparison of manual and automatic measures. We can observe that the tracker is not affected by the change of illumination from the contrast agent. The calcification is tracked correctly until the end of the sequence. We can observe also that when the calcification disappears, a failure of the tracking is detected (visible by the high peak in red color in Figure 6) and very fast after that event, the detector correctly reinitializes the target as soon as it reappears.

In Figure 8, mean, maximum and minimum displacement errors values that have been computed on the barycenters are represented for four real patient sequences. Sequences B and D present the highest maximum displacement errors, which are 3.9 mm and 4.5 mm, respectively. However, all tested fluoroscopic images showed that the mean displacement errors of the calcification tracking were less than 2mm. These error values remain within the clinical accepted range.

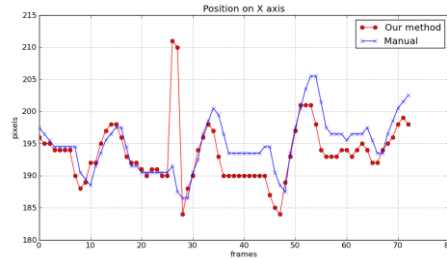


Figure 6. Projection of the calcification barycenter on X-axis compared to the manual curves.

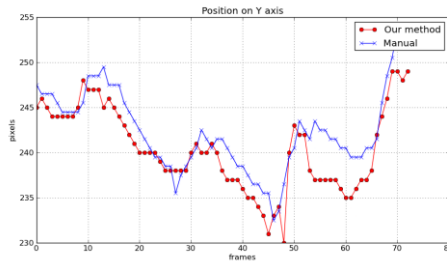


Figure 7. Projection of the calcification barycenter on Y-axis compared to the manual curves.

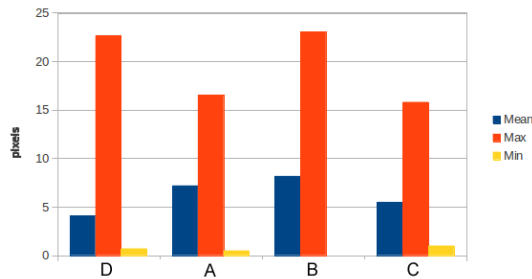


Figure 8. Displacement errors of the tracked calcification for four sequences.

The performance analysis of our approach is given in Table I for four patient image sequences.

TABLE I. PERFORMANCE ANALYSIS

Seq. name	Fr. Num.	Calcification		Performance	
		size	variance	recall	precision
A	59	16x19	69.57	0.717	0.717
B	195	19x29	45.60	0.897	0.897
C	80	31x25	53.77	1.000	1.000
D	74	15x18	47.61	0.945	0.945

The number of frames per sequence, the parameters that define the calcification template (size, grey level variance) and performance metrics (recall, precision) are given. In all four considered clinical cases, the detection rate was of 100%. We obtained high recall and precision values for most of the considered sequences. Nevertheless, more cases should be further performed to confirm these results, especially on cases of lower calcification or image quality. It is noticed that the bigger the size of initialized calcification template is, the greater recall/precision of the method is obtained. All sequences have the recall and precision values from 70% to 100%, which shows that this process can provide a good tracking of calcification over frames.

C. Conclusion

We proposed a robust approach to track the aortic valve calcifications in fluoroscopy imaging in order to determine the position of the aortic valve plane in intra-operative TAVI procedure. A minimal user-interaction is required to initialize the algorithm. The method has been tested on four patient image sequences and a quantitative evaluation has been performed. This approach has been developed to track calcifications but it can be applied also on other structures of interest. The method seems to be robust despite some difficulties that can arise during the image acquisition (occlusions, contrast variations). It provides very encouraging results for a clinical use to assist the positioning and deployment of the aortic valve bioprosthesis under live 2D fluoroscopic guidance.

REFERENCES

- [1] Yan, T. D., Cao, C., Martens-Nielsen, J., Padang, R., Ng, M., Valley, M. P. & Bannon, P. G. Transcatheter Aortic Valve Implantation for High-Risk Patients with Severe Aortic Stenosis: A Systematic Review. *The Journal of thoracic and cardiovascular surgery*, Vol.139, No.6, 2010, pp. 1519-28, ISSN 0022-5223.
- [2] Thomas, M., Schymik, G., Walther, T., Himbert, D., Lefevre, T., Treede, H., Eggebrecht, H., Rubino, P., Michev, I., Lange, R., Anderson, W. N. & Wendler, O. Thirty-Day Results of the SAPIEN Aortic Bioprosthesis European Outcome (SOURCE) Registry: A European Registry of Transcatheter Aortic Valve Implantation Using the Edwards SAPIEN Valve *Circulation*, Vol. 122, No.1, 2010, pp. 62-69.
- [3] Cribier A, Eltchaninoff H, Bash A, Borenstein N, Tron C, Bauer F, et al. Percutaneous transcatheter implantation of an aortic valve prosthesis for calcific aortic stenosis: first human case description. *Circulation*. 2002; 106(24):3006-8.
- [4] Wijesinghe N., Masson J., Niellispach F., Tay E., Gurvitch R., Wood D., Webb J. A Novel Real-Time Image Processor to Facilitate Transcatheter Aortic Valve Implantation. *Journal Am Coll Cardiol*; volume 55, issue 10s1, 2010.
- [5] Esmail Karar M., Holzhey D., John M., Rastan A., Mohr FW. and Burgert O. Image-Guided Transcatheter Aortic Valve Implantation Assistance System, Aortic Valve, Prof. Chen Ying-Fu (Ed.), ISBN: 978-953-307-561-7, InTech.
- [6] Maggio E. and Cavallaro A. *Video Tracking: Theory and Practice*. Wiley, 2011.
- [7] Kalal Z., Matas J., and Mikolajczyk K. Online learning of robust object detectors during unstable tracking. In *Proceedings of the IEEE On-line Learning for Computer Vision Workshop*, 2009, pp 1417–1424.
- [8] Lepetit V., Lagger P., and Fua P. Randomized trees for Real-Time keypoint recognition. In *IEEE Computer Society Conference on Computer Vision and Pattern Recognition*, Los Alamitos, CA, USA, vol. 2, 2005, pp 775–781.
- [9] Kalal Z., Mikolajczyk K., and Matas J. Forward-Backward Error: Automatic Detection of Tracking Failures. In *International Conference on Pattern Recognition*, 2010, pp 23–26.
- [10] Lucas B. D. and Kanade T. An iterative image registration technique with an application to stereovision. In *Proceedings of the International Joint Conference on Artificial Intelligence*, 1981, pp 674–679.
- [11] Stanley T. Birchfield and Shrinivas J. Pundlik. Joint Tracking of Features and Edges. *IEEE Conference on Computer Vision and Pattern Recognition (CVPR)* Anchorage, Alaska, 2008.